FERMILAB-PUB-05-333-AD

Transverse and longitudinal beam dynamics studies at the Fermilab photoinjector

J.-P. Carneiro,* N. Barov,† H. Edwards, M. Fitch,‡ and W. Hartung§
Fermi National Accelerator Laboratory, Batavia, Illinois 60510, USA

K. Floettmann and S. Schreiber
DESY, Hamburg, Germany

M. Ferrario
INFN-LNF, Frascati, Italy
(Received 2 October 2004; published 8 April 2005)

The Fermilab photoinjector produces electron bunches of 1–12 nC charge with an energy of 16–18 MeV. Detailed measurements and optimization of the transverse emittance have been carried out for a number of beam line optics conditions, and at a number of beam line locations. The length of the bunches has also been measured, first for an uncompressed beam (as a function of the charge) and then for a compressed beam of 8 nC charge (as a function of the 9-cell cavity phase). These measurements are presented and compared with the simulation codes HOMDYN and ASTRA.

PACS numbers: 29.25.Bx, 52.59.Sa, 41.60.Cr

I. INTRODUCTION

Fermilab, in collaboration with UCLA, INFN Milano, DESY, LAL Orsay, IPN Orsay, CEA Saclay, the University of Rochester, and Cornell University, has developed a rf photoinjector to produce high bunch charge (8 nC) with low normalized transverse emittance (< 20 mm mrad) in trains up to 600 bunches separated by 1 μs. The photoinjector is operated in partnership with the Northern Illinois Center for Accelerator and Detector Development. Two duplicate photoinjectors were built. The first was in operation from 1998 to 2002 at the TESLA Test Facility accelerator (TTF) at DESY [1]; this photoinjector was used to drive the TTF free electron laser (TTF-FEL) into saturation [2]. The second photoinjector is installed in the A0 building at Fermilab for photoinjector research and development and to study novel applications of high-brightness, pulsed electron beams. The goal of the studies presented in this paper is to characterize the beam produced by the Fermilab photoinjector.

II. EXPERIMENTAL LAYOUT

Figure 1 shows the photoinjector gun after installation at Fermilab. It consists of a 1.625-cell rf gun resonating in the $TM_{010}\pi$ mode at 1.3 GHz. The gun contains a high quantum efficiency Cs_2Te photocathode. The UV light is provided by a pulsed neodymium-doped yttrium lithium fluoride (Nd:YLF) laser [3]. To confine the space charge dominated beam, three solenoids are installed around the gun (a primary, a secondary, and a bucking solenoid to zero the magnetic field on the cathode). The beam is accelerated by a 9-cell superconducting TESLA cavity up to 16–18 MeV. After the 9-cell cavity, a magnetic chicane consisting of four dipoles may be used to compress the beam longitudinally. A quadrupole doublet and three quadrupole triplets are used to transport the beam to a spectrometer at the end of the beam line ($z \cong 11.2$ m, with z being the distance along the beam line and setting $z = 0$ at the cathode).

The predicted performance of the photoinjector is given in the TTF design report [4]. For the measurements discussed in this paper, the rf gun pulse length was 30 μs, the repetition rate was 1 Hz, and a train of 10 bunches was used, with charge between 1 and 12 nC per bunch. A laser pulse stacker was used to combine four short laser UV pulses (with a 4.3 ps FWHM Gaussian longitudinal distribution each) leading to a quasi-flattop UV pulse on the photocathode. The flattop duration was 10.7 ps FWHM as measured with a streak camera. The transverse size of the UV pulse on the photocathode was adjusted using a remotely controlled iris positioned at the entrance to the rf gun. A fraction of the UV light was reflected onto a screen so that the laser spot could be viewed at a position equivalent to the cathode location with a charge-coupled device camera. The images of the UV pulses on the screen showed a nonperfectly uniform transverse distribution, with intensity fluctuations of order $\pm 10\%$.

In this paper, the launch phase ϕ_0 of the rf gun is relative to the zero-crossing phase of the rf seen by the tail of the bunch while the phase ϕ_s of the 9-cell superconducting cavity is relative to acceleration on crest. The 9-cell cavity was operated with a flattop pulse length of 100 μs and an

*Corresponding author.
Electronic address: carneiro@fnal.gov
†Present address: Far-tech Inc., San Diego, CA 92121, USA.
‡Present address: Johns Hopkins University, Applied Physics Laboratory, MD 20723, USA.
§Present address: National Superconducting Cyclotron Laboratory, Michigan State University, East Lansing, MI 48824, USA.

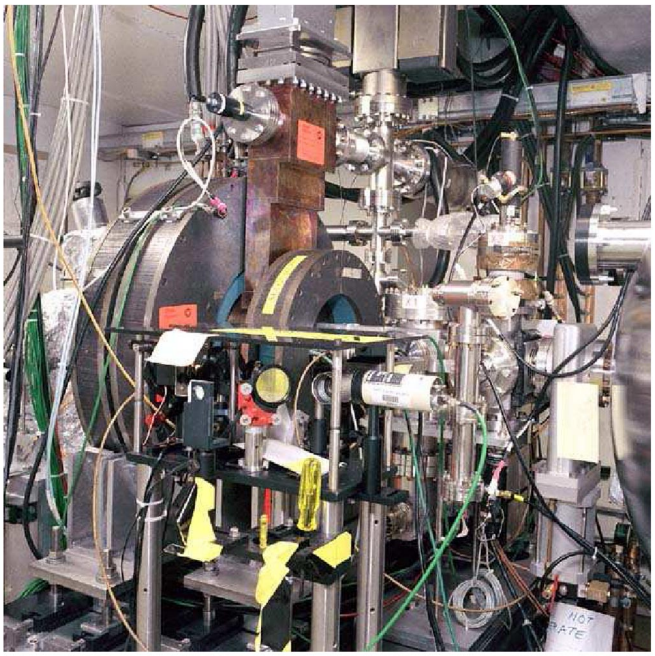

FIG. 1. (Color) The Fermilab rf gun. A small optical table for transport of the laser beam can be seen in the foreground, with the iron yokes for the three solenoids behind it. The waveguide feed for the rf gun is between the primary and secondary solenoids. The first two diagnostic ports of the beam line are to the right of the secondary solenoid; the edge of the cryostat for the 9-cell cavity is at the far right.

accelerating field of 12 MV/m. For most of the measurements, we set $\phi_s = -10°$ to minimize the energy spread. For a peak rf field at the cathode of $E_0 = 40$ MV/m and a launch phase of $\phi_0 = 40°$ to maximize the energy at the exit of the gun, the total energy E_t and the relative energy spread δ of a 1 nC uncompressed beam were then measured at $E_t = 18.2$ MeV and $\delta = 0.25\% \pm 0.02\%$. The relative energy spread δ is defined as the ratio of the rms energy spread to the total energy E_t. In the following, Q is the charge per bunch, σ is the rms size (x or y) of the laser beam on the cathode, and $B_z^{\max}$ is the maximum axial magnetic field. All three solenoids were used with the same current, which produces a nonzero magnetic field on the cathode (< 9 mT).

III. EMITTANCE DEFINITION

In this paper, the normalized rms emittance is defined by [5]

$$\epsilon_{n,\mathrm{rms}} = \beta\gamma\sqrt{\langle u^2\rangle\langle (u')^2\rangle - \langle uu'\rangle^2}, \tag{1}$$

where βc is the velocity of the beam, γ is the Lorentz factor, u and u' are the transverse coordinate and divergence of x or y, and $\langle\,\rangle$ denotes a rms value. Equation (1) defines the normalized trace-space emittance, which is equivalent to the normalized rms emittance for beams with small energy spread [6]; this i case for the studies presented in this paper.

IV. SIMULATION CODES

The beam dynamics simulations presented in this paper have been carried out with two codes: HOMDYN [7] and ASTRA [8].

A. HOMDYN

HOMDYN describes each bunch as a uniformly charged cylinder whose length and radius can vary under a self-laminar time evolution, keeping the charge distribution uniform inside the bunch. Each cylinder is divided into cylindrical slices of uniform size (multislice approximation), each one subject to the internal space charge fields (linear component) and external electric and magnetic fields. For a cylinder of radius R, HOMDYN uses the equivalence $u = R/2$ in Eq. (1) to compute the rms emittance $\epsilon_{n,\mathrm{rms}}$ with the rms performed over the total number of slices.

The model does not include a realistic treatment of the initial momentum distribution of the beam and the evolution in the momenta as the particles are extracted from the solenoidal field. The effect on the emittance is included approximately by adding two additional terms in quadrature, the normalized rms ''thermal emittance'' $\epsilon_{n,\mathrm{rms}}^{\mathrm{th}}$ due to the nonzero temperature of the electrons emitted from the photocathode and the normalized rms ''magnetic emittance'' $\epsilon_{n,\mathrm{rms}}^{\mathrm{mag}}$ proportional to the residual magnetic field on the photocathode. These quantities are obtained via [9]

$$\epsilon_{n,\mathrm{rms}}^{\mathrm{th}} = \frac{R_0}{2}\sqrt{\frac{2E_{\mathrm{kin}}}{m_0c^2}}\frac{1}{\sqrt{3}} \tag{2}$$

and [10]

$$\epsilon_{n,\mathrm{rms}}^{\mathrm{mag}} = \frac{eR_0^2B_0}{8m_0c}, \tag{3}$$

where R_0 is the radius of the laser beam (considered as uniformly distributed); E_{kin} is the kinetic energy of the electrons emitted from the photocathode which we assume to be 0.75 eV; B_0 is the residual magnetic field at the photocathode. For $R_0 = 1.5$ mm and $B_0 = 6.7$ mT (typical 1 nC operation), we obtain $\epsilon_{n,\mathrm{rms}}^{\mathrm{th}} \cong 0.7$ mm mrad and $\epsilon_{n,\mathrm{rms}}^{\mathrm{mag}} \cong 1.1$ mm mrad.

B. ASTRA

ASTRA is a macroparticle code which tracks particles through external electric and magnetic fields, taking into account the space charge field (linear and nonlinear) of the particle cloud. The initial transverse and longitudinal particle distribution is read from an external file and can be arbitrarily defined by the user. For most of the simulations presented in the following, we used 5×10^3 macropar-

ticles. ASTRA computes the normalized rms emittance as defined by Eq. (1). The initial distribution accounts for the temperature of the electrons emerging from the cathode, assuming the electrons are emitted with $E_{\rm kin} = 0.75$ eV; the evolution of the momenta is calculated explicitly as the beam travels through the solenoidal field. Hence it is not necessary to add thermal and magnetic emittance values in quadrature.

C. Methodology

The laser pulse duration was 11 ps for HOMDYN; in ASTRA we assumed a flattop of 11 ps with rising edges of 1.9 ps. The transverse laser distribution was assumed perfectly uniform in both codes. The external input files were produced using SUPERFISH [11] for the rf gun and the code FEM [12] for the 9-cell cavity. For each set of currents in the solenoids, we produced an external input file using POISSON [11]. The external electric and magnetic field input files were identical for HOMDYN and ASTRA.

V. TRANSVERSE BEAM DYNAMICS

A. Emittance measurement principle

The emittance measurements were done using the slit technique: five actuator-mounted slit masks were used to measure the vertical emittance (ϵ_y) at $z = 3.8$ m, and both emittances (ϵ_x and ϵ_y) at $z = 6.5$ and 9.6 m. The beamlets passing through the slits are viewed with optical transition radiation (OTR) screens located at a distance $d = 384$, 1122, and 380 mm from the slits, respectively. The masks consist of 6 mm thick tungsten slats with 50 μm wide slits spaced 1 mm apart. The rms normalized emittance was computed using the relation

$$\epsilon_{n,\mathrm{rms},u} = \beta\gamma\sigma_u\sigma'_{u,\mathrm{slits}}, \tag{4}$$

where σ_u is the rms size of the beam at the slit location and $\sigma'_{u,\mathrm{slits}}$ the divergence of the beam measured as the ratio of one slit rms size divided by the distance d between the slit mask and the OTR screen. A Gaussian fit was used to obtain σ_u and $\sigma'_{u,\mathrm{slits}}$. All the results presented in this paper were obtained using Eq. (4). With this method of analyzing the slit image, we assume that the transverse phase space of the beam is Gaussian. Thus, nonlinear effects due to non-Gaussian beams are not taken into account in this analysis. Beams with non-Gaussian tails can be a significant source of emittance increase, as discussed in the following sections.

B. Emittance optimization

All the measurements presented in this section were done at $z = 3.8$ m, at the exit of the 9-cell cavity.

Figure 2 shows ϵ_y as a function of charge. Measurements were done for $Q = 0.25$, 1, 4, 6, 8, and 12 nC with $\phi_0 = 40°$ and $E_0 = 40$ MV/m. The choice of launch phase stems from a previous optimization study [13]; the peak field at the cathode is set close to the maximum available. For each charge, we measured the emittance for different values of the laser spot size σ on the cathode and as a function of the solenoid current and we indicate in Fig. 2 the minimum obtained. Thus, the optimized emittance measured at the exit of the injector has an approximately linear dependence on the charge. A linear dependence on the charge has already been observed for different charges and rf gun operating frequencies; examples include Brown *et al.* (10–50 pC, 17 GHz) [14], Schmerge *et al.* (50–350 pC, 2.856 GHz) [15], Bossart *et al.* (1–20 nC, 3 GHz) [16], and Guimbal *et al.* (1–10 nC, 144 MHz) [17].

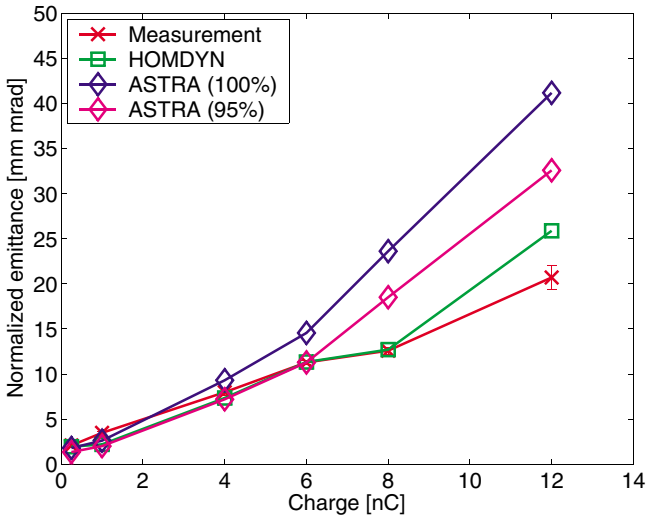

FIG. 2. (Color) Comparison of the measured and simulated minimum normalized vertical emittance at $z = 3.8$ m as a function of the charge per bunch.

The minimum transverse emittance of a 1 nC beam measured with the Fermilab gun both at Fermilab and DESY [18] was 3.5 ± 0.1 mm mrad. This measured value of the emittance is not an absolute minimum. According to HOMDYN and ASTRA, a transverse emittance of 1.2 mm mrad can be produced by the Fermilab rf gun operating at 40 MV/m, using a laser pulse with a flattop of 20 ps, an accelerating field on the 9-cell cavity of 12.5 MV/m, and adjusting the bucking solenoid to zero the magnetic field on the cathode. The simulations also predict that the emittance can be decreased to 0.9 mm mrad by operating the rf gun at 60 MV/m. An experiment is ongoing at the Photo-Injector Test Facility at DESY Zeuthen [19] to reduce the emittance to this value with a rf gun operating at 1.3 GHz and 60 MV/m; this is one of the goals for the European x-ray FEL [20]. Note that a transverse emittance of 1.2 mm mrad has been demonstrated with a 1 nC beam in an *S*-band rf gun (Sumitomo Heavy Industry, Japan [21]) using a square temporal laser pulse shape of 9 ps FWHM, a peak electric field on the rf gun of 100 MV/m, and a total beam energy of 14 MeV.

This is reported as the smallest emittance produced so far [22].

We showed in Fig. 2 the predictions of ASTRA taking 100% and 95% of the beam for the computation of the rms normalized emittance. From Fig. 2, we can see that HOMDYN and ASTRA agree with the experimental results for a charge up to 4 nC. A good agreement between the measured transverse emittance of 1.0 nC bunches with ASTRA is also presented in Ref. [23]. References [14,15] show a good agreement at low charges (< 0.4 nC) between the measured transverse emittance and simulations performed with the particle tracking code PARMELA. Previous simulations [24] have shown an excellent agreement between HOMDYN, ASTRA, and PARMELA for an *S*-band rf gun operating at 1 nC. This paper is the first to compare measurements of the transverse emittance to ASTRA and HOMDYN for charges above 1 nC. From Fig. 2, we see that ASTRA disagrees with the measured emittance and HOMDYN for charges higher than 4 nC, more so for the 100% emittance than the 95% cases. A comparison between measured transverse emittances and PARMELA for charges from 1–20 nC is presented in [16] and the measured emittance is systematically higher than the simulations, an effect which is reported as not understood.

Figure 3(a) shows the image of the 8 nC beam going through the slits and Fig. 3(b) shows the density projection. A Gaussian fit of the beamlet of highest intensity is shown in Fig. 3(c). From this image, the beam appears Gaussian. Our conclusion is that either the emittance measurement of a high charge beam needs to be improved in order to better detect the tails of the beam or the transverse emittance predicted by ASTRA for high charges is overestimated.

C. Emittance along the beam line

Table I shows the emittance of 1 and 8 nC beams measured in three locations along the beam line as compared with HOMDYN and ASTRA. We used the parameters of the rf gun and the 9-cell cavity that gave the minimum emittance at $z = 3.8$ m, as indicated in Fig. 2.

For the 1 nC case, $\sigma = 0.8$ mm, $B_z^{\max} = 0.132$ T, and we used the first triplet ($z = 6.1$—6.4 m) to optimize the transport until the end of the spectrometer. For the 8 nC case, $\sigma = 1.5$ mm, $B_z^{\max} = 0.126$ T, and we used the first and second triplet ($z = 7.8$—8.1 m) for the transport. Table I shows that the measured emittances of both the 1 and 8 nC beams increase along the beam line. HOMDYN and ASTRA predict emittances slightly lower in the 1 nC case. As discussed in [25], a possible source of emittance dilution is the transverse distribution of the laser beam which was taken as uniform in HOMDYN and ASTRA but has in reality some nonlinearity (see Sec. II). The 8 nC case shows a strong disagreement with ASTRA. A quadrupole scan was done at $z = 7.8$ m for a 1 nC beam to cross-check the measured values of the emittance [13]. We measured

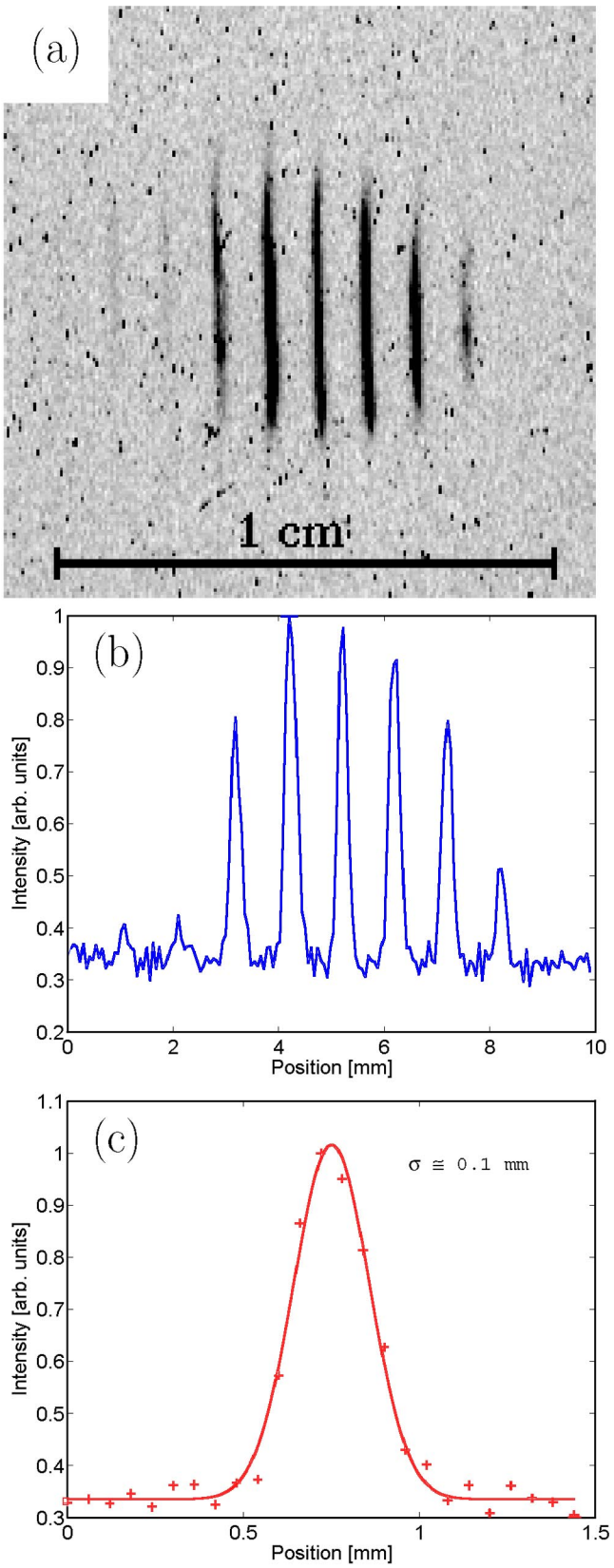

FIG. 3. (Color) (a) Image of an 8 nC beam going through the slit mask located 384 mm upstream, (b) density projection, and (c) Gaussian fit of the beamlet of highest intensity.

TABLE I. Emittance measurements for 1 and 8 nC beams at different locations along the beam line, with comparison to HOMDYN (H) and ASTRA (A) simulations.

		Emittance (mm mrad)					
	z	$Q = 1$ nC			$Q = 8$ nC		
Item	(m)	Meas.	H	A	Meas.	H	A
ϵ_y	3.8	3.5 ± 0.2	2.2	2.6	10.0 ± 0.1	12.7	22.9
ϵ_x	6.5	5.0 ± 0.2	2.3	2.3	11.6 ± 0.5	13.4	16.9
ϵ_y	6.5	5.1 ± 0.2	2.2	2.3	8.9 ± 0.7	12.3	16.4
ϵ_x	9.6	6.8 ± 0.2	2.3	3.2	14.4 ± 0.5	10.7	15.6
ϵ_y	9.6	5.8 ± 0.2	1.9	2.1	18.3 ± 0.9	13.8	16.2

$\epsilon_x = 4.2 \pm 0.1$ mm mrad and $\epsilon_y = 8.2 \pm 0.1$ mm mrad with the quadrupole scan, in approximate agreement with Table I.

VI. LONGITUDINAL BEAM DYNAMICS

A. Bunch length measurement principle

The bunch length measurements were done using a remotely controlled Hamamatsu streak camera with a resolution of 2 ps FWHM (as specified by the manufacturer, see [26]). The light from the OTR screen located at $z = 6.5$ m is transported to the slit of the streak camera located in the bunker, at approximately 2 m from the OTR screen. Prior to installation into the bunker, the streak camera was calibrated using the time difference between an UV beam going through air and a quartz plate [27].

The bunch length was determined by a quadratic subtraction of the rms size of the signal given by the camera operated in static mode and streak mode. The rms size of the signal was obtained using a Gaussian fit of the camera picture.

B. Bunch length versus charge

Figure 4 shows the measurement of the bunch length as a function of the charge, in good agreement with HOMDYN and ASTRA. For these measurements, we used $\sigma = 2$ mm, $E_0 = 40$ MV/m, $\phi_0 = 40°$, and $\phi_s = -10°$. The chicane was degaussed and turned off. The charge was measured by an integrating current transformer. The plots show the average value of the charge and bunch length for five shots. The bunch length is seen to grow linearly with charge. This linear dependence has been observed by Dowell *et al.* [28] for charges between 15 and 300 pC with a rf gun operating at 2.856 GHz.

The normalized brightness can be defined for a Gaussian beam as [29]

$$B_n = \frac{\hat{I}}{\epsilon_{n,x}\epsilon_{n,y}}, \tag{5}$$

where $\hat{I} = \frac{cQ}{\sqrt{2\pi}\sigma_z}$ is the peak current and $\epsilon_{n,x}$ and $\epsilon_{n,y}$ are the normalized rms emittances in x and y, respectively. For a

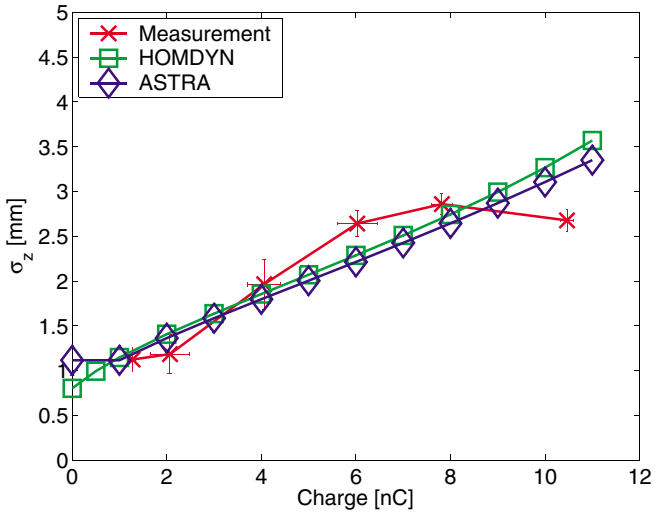

FIG. 4. (Color) Comparison of the measured and simulated bunch length as a function of the charge per bunch.

1 nC beam at Fermilab, the results reported in Fig. 4 and Table I lead to $B_n = (9.0 \pm 0.6) \times 10^{12}$ A/(mm mrad)^2. For comparison, Ref. [30] states that the highest brightness values achieved in operating photoinjectors are of order 10^{13} A/(mm mrad)^2.

C. Magnetic compression

To achieve compression in the chicane, the beam must have an energy-phase correlation such that the head of the bunch has a lower energy than the tail at the entrance to the chicane. Under this condition, particles in the tail of the bunch travel a shorter path through the chicane than particles in the head, producing longitudinal compression. The energy-phase correlation is obtained by decreasing the phase of the 9-cell cavity with respect to the phase of minimum energy spread ($\phi_s = -10°$).

Figure 5 shows the measurement of the rms length of an 8 nC beam as a function of the phase ϕ_s of the 9-cell cavity. These measurements are in good agreement with HOMDYN (it is not possible to simulate a magnetic chicane with ASTRA at the moment).

The injector parameters used for this measurement are the ones given in Sec. VI B except for the size of the laser beam ($\sigma = 2.3$ mm) and the current in the solenoids ($B_z^{\max} = 0.130$ T). The current in the chicane was set empirically, with the first and fourth dipole powered at -2.02 A ($|B_y| \cong 67.3$ mT) and the second and third at $+2.12$ A ($|B_y| \cong 70.6$ mT). The total energy of the beam was measured at $E_t = 17.9$ MeV, in good agreement with HOMDYN (17.5 MeV). A 3D model of the chicane has been constructed [31] using the electromagnetic code OPERA [32]. For these parameters, OPERA predicts a bending angle of the beam going into the magnetic chicane of $\sim 22.8°$, close to the theoretical angle of 22.5°. OPERA indicates also that the inner dipoles need to be powered with a higher

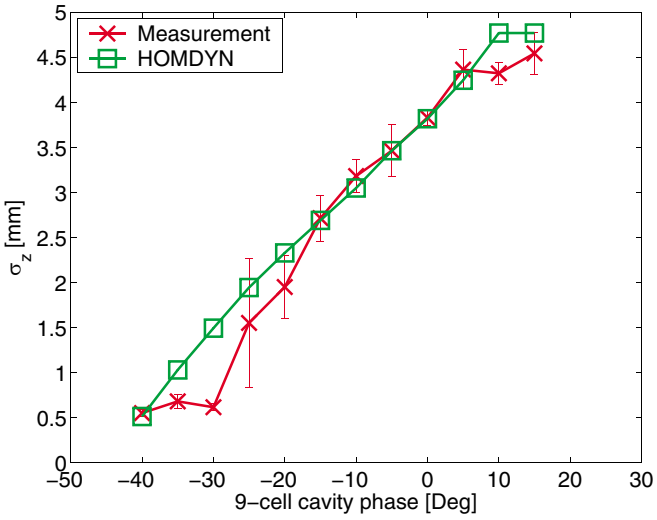

FIG. 5. (Color) Measured and simulated compression of an 8 nC beam as a function of the 9-cell cavity phase. The $\phi_s = 0$ corresponds to acceleration on crest.

current (5%–10%) than the outer ones to compensate for the fringe fields generated by the first and last dipoles, consistent with the empirically chosen settings.

The phase of the 9-cell cavity reported in Fig. 5 that gives the minimum energy spread is $\phi_s = -10°$. For this phase, the dipoles of the chicane do not affect the length of the bunch. We measured a rms bunch length comparable to the length indicated in Fig. 5 for a 8 nC bunch going through the degaussed chicane.

For ϕ_s below that of the minimum energy spread, we observed compression of the bunches. As indicated in Fig. 5, the maximum compression was measured at $\phi_s = -30°$. At maximum compression, the peak current was measured as 1.7 kA, with a total energy of 14.7 MeV, in good agreement with HOMDYN (15.4 MeV). For $\phi_s < -40°$, full transmission of the beam could not be achieved.

As shown in Fig. 5, we measured an elongation of the bunch for $\phi_s > -10°$. When the phase increases, the 9-cell cavity inverses the energy-phase correlation such that the head of the bunch has an energy higher than the tail.

The measurements were repeated with different charges ($Q = 1$, 4, 6, 8, and 12 nC) and laser pulse lengths ($\sigma_t =$ 1.8 and 4.6 ps). These results, presented in Ref. [27], are in good agreement with the ones discussed here. The maximum peak current measured was 2.8 kA, obtained by compression of a 12 nC beam to $\sigma_z = 0.6$ mm.

Work is in progress at Fermilab to measure the emittance of a compressed beam. A first attempt was made for a 1 nC beam, operating the photoinjector remotely from DESY [31]. We observed an energy modulation of the beam, which we believe is due to coherent synchrotron radiation effects [33] as the beam travels through the chicane. We also observed that the emittance of a compressed beam was not significantly larger than that of the uncompressed beam. More measurements must be done to confirm these results.

VII. CONCLUSION

We have determined the parameters of the Fermilab photoinjector that produce a low emittance beam for charges of 1–12 nC. The vertical emittance has been measured at the exit of the 9-cell cavity ($z = 3.8$ m): $\epsilon_y = 3.5 \pm 0.1$ mm mrad and $\epsilon_y = 20.7 \pm 1.3$ mm mrad for charges of 1 and 12 nC, respectively. The measured minimum emittance increases linearly with the charge. For a beam with a charge up to 4 nC, ASTRA agreed well with HOMDYN and with the measured transverse emittance; for higher charges, ASTRA differed from the others. It is important to note that the measured values of the transverse emittance are not absolute minima.

We measured an increase in the transverse emittance along the beam line by a factor of ~1.5 (for 1 and 8 nC), which is not predicted by HOMDYN or ASTRA. More studies must be done in order to understand the reason for this increase.

HOMDYN and ASTRA agreed well with the experimental results of the bunch length versus the charge. The bunch length of a compressed beam is also in good agreement with HOMDYN. The maximum compression factor (5–6) was obtained for a phase of the 9-cell cavity 30° lower than the one giving the minimum energy spread. Further studies of compressed beams are underway at Fermilab. Work is in progress to incorporate a magnetic chicane model into ASTRA.

ACKNOWLEDGMENTS

We thank our colleagues from A0 for their support during the operation of the accelerator. We would like also to thank D. Edwards and J. Le Duff for useful discussions and comments and P. Piot for careful reading of the paper.

[1] S. Schreiber, in *Proceedings of the 1999 Particle Accelerator Conference, New York*, edited by A. Luccio and W. MacKay (IEEE, Piscataway, NJ, 1999), pp. 84–86.
[2] V. Ayvazyan *et al.*, Eur. Phys. J. D **20**, 149 (2002).
[3] A. R. Fry, M. J. Fitch, A. C. Melissinos, and B. D. Taylor, Nucl. Instrum. Methods Phys. Res., Sect. A **430**, 180 (1999).
[4] DESY Report No. TESLA 95-01, 1995.
[5] P. M. Lapostolle, IEEE Trans. Nucl. Sci. **18**, 1101 (1971).
[6] K. Floettmann, Phys. Rev. ST Accel. Beams **6**, 034202 (2003).
[7] M. Ferrario and L. Serafini, in *Proceedings of the 6th European Particle Accelerator Conference (EPAC'98), Stockholm*, edited by S. Myers, L. Liljeby, C. Petit-Jean-Genaz, J. Poole, and K. G. Rensfelt (IOP, Bristol, 1999), pp. 1271–1273.

[8] K. Floettmann, ASTRA User's Manual, 2000, http://www.desy.de/~mpyflo/Astra_ dokumentation/

[9] K. Flöttmann, DESY Report No. TESLA-FEL 97-01, 1997.

[10] S. Nagaitsev and A. Shemyakin, Fermilab Technical Report No. TM-2107, 2000.

[11] POISSON/SUPERFISH group of codes, Los Alamos, Version 4.28 for PC, 2002.

[12] J. Sekutowicz, in *Proceedings of the 1994 International Linac Conference, Tsukuba, Japan*, edited by K. Takata, Y. Yamazaki, and K. Nakahara (KEK, Tsukuba, Japan, 1994), pp. 284–286.

[13] J.-P. Carneiro, Ph.D. thesis, Université Paris XI, Orsay, France, 2001.

[14] W. J. Brown, S. E. Korbly, K. E. Kreischer, I. Mastovsky, and R. J. Temkin, Phys. Rev. ST Accel. Beams **4**, 083501 (2001).

[15] J. Schmerge, P. Bolton, J. Clendenin, F.-J. Decker, D. Dowell, S. Gierman, C. Limborg, and B. Murphy, SLAC Report No. SLAC-PUB 8963, 2001.

[16] R. Bossart *et al.*, in *Proceedings of the 1995 Particle Accelerator Conference, Dallas, TX* (IEEE, Piscataway, NJ, 1995), pp. 719–721.

[17] J.-G. Marmouget, A. Binet, P. Guimbal, and J.-L. Coacolo, in *Proceedings of the Eighth European Particle Accelerator Conference (EPAC2002), Paris*, edited by T. Garvey, J. Le Duff, P. Le Roux, C. Petit-Jean-Genaz, J. Poole, and L. Rivkin (EPS-IGA and CERN, Geneva, 2002), pp. 1795–1797.

[18] P. Piot, S. Schreiber, D. Sertore, K. Flöttmann, A. Cianchi, and L. Catani, in *Proceedings of the 1999 Particle Accelerator Conference, New York* (Ref. [1]), pp. 86–88.

[19] F. Stephan *et al.*, in *Proceedings of the 2004 Free Electron Laser Conference, Trieste, Italy, 2004* (Sincrotrone Trieste, Trieste, 2004).

[20] R. Brinkmann, in *Proceedings of the XXII International Linear Accelerator Conference, Lübeck, Germany, 2004* (DESY, Hamburg, 2004).

[21] J. Yang, F. Sakai, T. Yanagida, M. Yorozu, Y. Okada, T. Nakajyo, K. Takasago, and A. Endo, in *Proceedings of the Eighth European Particle Accelerator Conference (EPAC2002), Paris* (Ref. [17]), pp. 1828–1830.

[22] P. Piot, in *Proceedings of the Joint ICFA Advanced Accelerator and Beam Dynamics Workshop on the Physics and Applications of High Brightness Electron Beams, Sardinia, Italy, 2002* (World Scientific, Singapore, 2003).

[23] M. Krasilnikov *et al.*, in *Proceedings of the Ninth European Particle Accelerator Conference (EPAC2004), Lucerne, 2004*, edited by J. Chrin, C. Petit-Jean-Genaz, J. Poole, C. Prior, and H.-A. Synal (EPS-IGA and CERN, Geneva, 2004), pp. 360–362.

[24] C. Limborg, Y. Batygin, M. Boscolo, M. Ferrario, V. Fusco, C. Ronsivalle, L. Giannessi, M. Quattromini, J. P. Carneiro, and K. Floetmann, in *Proceedings of the 2003 Particle Accelerator Conference, Portland, OR* (IEEE, Piscataway, NJ, 2003), pp. 3548–3550.

[25] F. Zhou, I. Ben-Zvi, M. Babzien, X. Y. Chang, A. Doyuran, R. Malone, X. J. Wang, and V. Yakimenko, in *Proceedings of the Eighth European Particle Accelerator Conference (EPAC2002), Paris* (Ref. [17]), pp. 275–277.

[26] Instruction manual for universal streak camera C5680, Hamamatsu, 1997.

[27] M. J. Fitch, Ph.D. thesis, University of Rochester, Rochester, New York, 2000.

[28] D. Dowell, P. Bolton, J. Clendenin, P. Emma, S. Gierman, C. Limborg, B. Murphy, and J. Schmerge, SLAC Report No. SLAC-PUB 9541, 2002.

[29] M. Reiser, *Theory and Design of Charged Particle Beams* (Wiley, New York, 1994).

[30] G. Suberlucq, in *Proceedings of the Ninth European Particle Accelerator Conference (EPAC2004), Lucerne, 2004* (Ref. [23]), pp. 64–68.

[31] J.-P. Carneiro, K. Flöttmann, P. Piot, N. Barov, K. Desler, D. Edwards, and M. Ferrario, in *Proceedings of the Eighth European Particle Accelerator Conference (EPAC2002), Paris* (Ref. [17]), pp. 1759–1761.

[32] OPERA 8.0, Vector Fields Limited, Oxford, England, 2001.

[33] M. Borland, Phys. Rev. ST Accel. Beams **4**, 070701 (2001).